



Deposited via The University of York.

White Rose Research Online URL for this paper:

<https://eprints.whiterose.ac.uk/id/eprint/95049/>

Version: Published Version

---

**Proceedings Paper:**

West, Andrew, van der Schans, Marc, Xu, Cigang et al. (2015) Optimisation of photoresist removal from silicon wafers using atmospheric-pressure plasma jet effluent. In: Proc 22nd ISPC.

---

**Reuse**

Items deposited in White Rose Research Online are protected by copyright, with all rights reserved unless indicated otherwise. They may be downloaded and/or printed for private study, or other acts as permitted by national copyright laws. The publisher or other rights holders may allow further reproduction and re-use of the full text version. This is indicated by the licence information on the White Rose Research Online record for the item.

**Takedown**

If you consider content in White Rose Research Online to be in breach of UK law, please notify us by emailing [eprints@whiterose.ac.uk](mailto:eprints@whiterose.ac.uk) including the URL of the record and the reason for the withdrawal request.

## Optimisation of photoresist removal from silicon wafers using atmospheric-pressure plasma jet effluent

A.T. West<sup>1</sup>, M. van der Schans<sup>2</sup>, C. Xu<sup>3</sup>, T. Gans<sup>1</sup>, M. Cooke<sup>3</sup> and E. Wagenaars<sup>1</sup>

<sup>1</sup> York Plasma Institute, Department of Physics, University of York, York, U.K.

<sup>2</sup> Department of Applied Physics, Eindhoven University of Technology, the Netherlands

<sup>3</sup> Oxford Instruments Plasma Technology, Bristol, U.K.

**Abstract:** Atmospheric-pressure plasma jets (APPJs) can offer high-quality etch of photoresist at rates up to 10  $\mu\text{m}/\text{min}$ , compared to 10 - 100  $\text{nm}/\text{min}$  using traditional low-pressure methods, while avoiding the inconveniences of operating vacuum systems. We determined that the removal rate of photoresist is strongly linked with the flux of atomic oxygen in the APPJ effluent as measured using laser-based diagnostics (TALIF).

**Keywords:** atmospheric-pressure plasma jet, photoresist, ashing, etching

### 1. Introduction

The manufacture of semiconductor devices relies on photoresist to act as a mask during plasma etching to achieve architectures on the nanoscale at a high aspect ratio. Photoresist comprises of organic chain molecules which lithography then imprints a pattern into, leaving the photoresist layer preferentially softened or hardened. The micron or more thick layer of hardened and softened areas allow a plasma process to etch faster through the soft layers and into the underlying wafer, whereas the hardened layer acts as a sacrificial surface which remains partially intact, protecting the substrate underneath. The photoresist mask must be removed and reapplied multiple times during the manufacturing cycle to build up the architecture on the substrate. Low-pressure oxygen plasmas are often preferred to remove photoresist over wet chemical solvents, but their slow removal rates on the order of 10 - 100  $\text{nm}/\text{min}$  [1] and requirement for vacuum equipment does not make them conducive to rapid continuous production. In addition, direct plasma photoresist removal, known as plasma ashing, can cause damage through ion bombardment at the surface of the wafer, and the electric fields that develop on the surface due to sheath formation can affect sensitive structures such as transistor gates.

Atmospheric-pressure plasma jets (APPJs) offer not only a non-vacuum plasma solution, but also faster removal rates than low-pressure plasmas. To avoid the associated issues of sheath formation at the surface of the wafer, a plasma effluent can be used instead. The active plasma can form the rich radical chemistry required, then the plasma is allowed to recombine at the outlet nozzle, leaving the neutral reactive species to be transported in the gas flow to chemically etch the surface.

It has been determined that for low-pressure plasma ashing, atomic oxygen has a link to etch rate [2], with higher concentrations of atomic oxygen leading to higher etch rates of photoresist. This gives a direction in which to get optimal ashing rates in the atmospheric plasma by

tailoring parameters to increase atomic oxygen density. Various parameters were investigated, such as driving frequency, input power, flow rate, gas composition and distance from nozzle to substrate. The use of Two-photon Absorption Laser Induced Fluorescence (TALIF) allows for a measure of the relative atomic oxygen densities and how they compare to the observed etch rate of photoresist. Attenuated Total Reflectance Fourier Transform Infrared Spectroscopy (ATR FTIR) is used to assess the quality of etch after treatment. The atmospheric-plasma treated substrates are compared to traditional ICP low-pressure plasma treatment to investigate signs of residual photoresist left of the surface.

### 2. Experimental design

The atmospheric-pressure plasma jet is operated using 13.56 MHz and also 40.68 MHz radio frequency (RF) voltages. Helium gas with admixtures of up to 1% oxygen are passed through the device and driven into a plasma state between the electrodes. The plasma recombines at the outlet to open air leaving the radical rich effluent to interact with the surface, see Fig. 1. The jet is placed with the nozzle facing vertically downwards at a sample surface. The device has quartz windows to give a view of the plasma, and is designed for access by optical diagnostics [3, 4], which has allowed for characterisation of its chemistry [5, 6].

Etch rates are measured by first analysing the thickness of photoresist using a surface profile analyser. Once the photoresist thickness is characterised, the time taken to etch through the photoresist to reveal the silicon wafer underneath is recorded, and from these two quantities, the rate is calculated. Two different photoresists are used: AZ 9260 at a thickness of 7.5  $\mu\text{m}$  and S1813 at a thickness of 1.5  $\mu\text{m}$  on the substrate as per the manufacturer's recommendation. Etch rate is assessed as a function of input parameters, for example input RF power. TALIF measurements then give a measure of the atomic oxygen density at the nozzle exit to see if trends

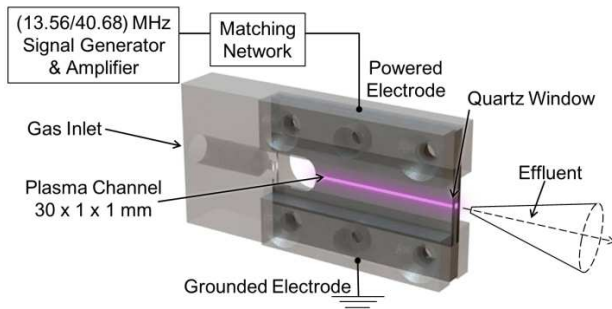


Fig. 1. Diagram of APPJ. Helium with admixtures of oxygen passes through the plasma channel, where at the nozzle the plasma recombines leaving a neutral effluent.

indicate the correlation of atomic oxygen to etch rate as is seen at low-pressure.

Previous measurements of atomic oxygen density for biomedical applications using TALIF and modelling give a basis on which to tailor the plasma jet. Measurements reveal that 0.5% oxygen admixture yields the greatest atomic oxygen concentration [7, 8]. These measurements also indicate that the closer the jet nozzle, the higher the O concentration, with a rapid reduction in concentration as the distance is increased. At distances similar to the electrode gap (less than 2.5 mm) a discharge begins to form between the powered electrode and the surface which acts as a ground. This is unwanted, as direct plasma formation on the surface will develop sheath structures and therefore the issues with ion impact damage and electric fields. This restriction leads to an optimum safe nozzle to substrate distance of 3 mm.

### 3. Results and discussion

Preliminary tests showed that 0.5% oxygen admixture will yield the highest etch rate at 13.56 MHz voltages and that with increased distance from the nozzle there is a dramatic drop in etch rate also at 13.56 MHz. With small input powers, etch rates were around 75 nm/min, comparable with traditional low-pressure etching. An immediate increase in etch rate came with an increased driving frequency of 40.68 MHz. The third harmonic of 13.56 MHz outperformed the fundamental in all measurements. For example the 75 nm/min starting rate was increased to 125 nm/min, and tests showed consistently a roughly a two-thirds increase in etch rate at 40.68 MHz over 13.56 MHz.

TALIF measurements along with modelling show a linear dependency on atomic oxygen densities as input power increases [8-10]. The etch rates mirror this trend, and with increasing input power from the RF generator there is an increase in etch rate as shown in Fig. 2. Maximum photoresist removal rates are now close to 1  $\mu\text{m}/\text{min}$ . Unfortunately, power cannot be increased indefinitely; eventually the plasma transitions into an arcing mode and causes damage to the device.

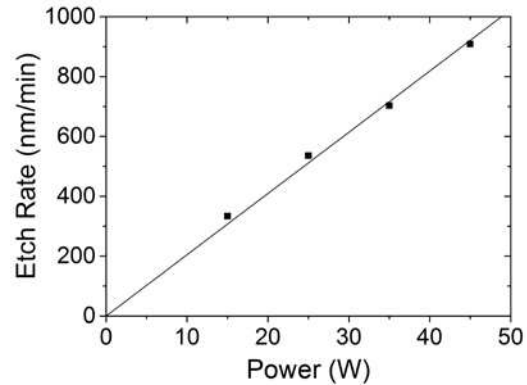


Fig. 2. Etch rate of photoresist as a function of generator input power at 40.68 MHz. The linear dependency mimics that of atomic oxygen density with input power.

Atomic oxygen flux appears to be a good indicator for etch rate of photoresist, and so further optimisation can be made by investigating how atomic oxygen flux can be increased to the surface. An obvious method is to increase the flow rate of precursor gas as to increase the rate at which species are transported to the surface. This can only work if the rate of atomic oxygen production does not decrease to any great extent with increased flows. In Fig. 3, TALIF measurements show only a decrease of around 10 - 15% in the relative O density up to 4.5 slm. This results in an approximately linear increase of O flux to the substrate surface with respect to flow rate increase. Fig. 4 shows how the etch rate increases in line with the expected flux.

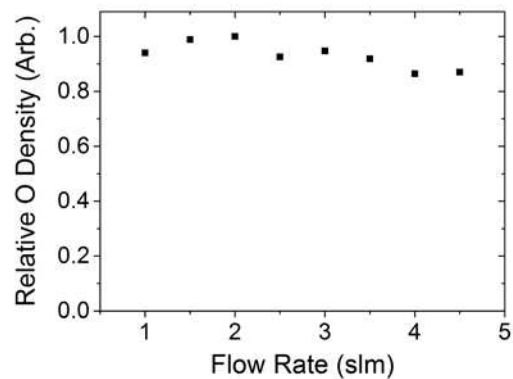


Fig. 3. TALIF measurements show a consistent O density with flow rate; only a 10 - 15% change.

An increase in flow rate also suffers from limitations as with input power. As flow rate increases, the gas flow velocity increases, and at 10 slm the etch pattern becomes distorted and no longer resembles a circular shape, rather it becomes non-uniform and patchy.

With increased flow, etch rates can approach 2  $\mu\text{m}/\text{min}$ , yet when the substrate is heated to around the glass temperature of photoresist at  $\sim 100^\circ\text{C}$  the etch rate is greatly enhanced to 10  $\mu\text{m}/\text{min}$ . Heating the wafer is a

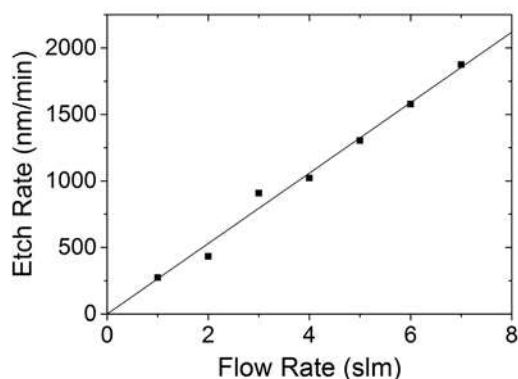


Fig. 4. As flow rate increases the O flux reaching the surface is increased and results in faster etch rates.

technique used currently to increase ashing rates [11]. Most atmospheric pressure devices have achieved etch rates on the order of hundreds of nm/min [13-15]. Rates close to  $\mu\text{m}/\text{min}$  have been achieved for the same etch area as this study, but at the expense of ten times the gas and power [12].

The power reported in Fig. 2 and compared to [12] is from the RF generator and not the plasma power. The power that is deposited into the plasma may be as much as an order of magnitude less than the generator power.

The radio frequency systems used to drive the plasma use L-type or Pi-type matching networks to offer impedance matching between the jet and the generator. As seen in Fig. 5, in the linear regime of a normal glow-mode, the plasma power is between 0.5 and 4 W, when compared to 20 - 40 watts generator power, clearly generator power overestimates how much energy is required to operate an APPJ. The generic L and Pi type RF matching networks used are lossy compared to custom made inductive shunts. A less flexible but more efficient matching design can reduce the overall power consumption in a smaller form factor [16].

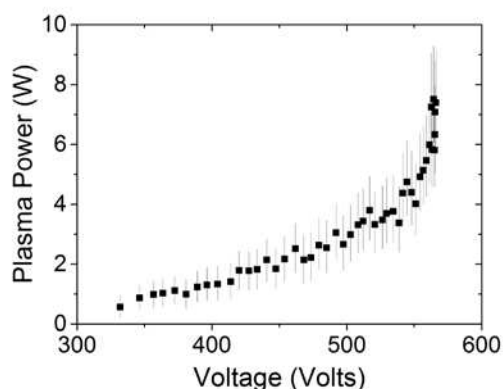


Fig. 5. Plasma power measured at 13.56 MHz as a function of applied voltage near the electrodes. The jet is operated in the linear regime of the normal glow-mode (<550 Volts) rather than the transition to gamma-mode.

Though the etch rate is comparable to the highest found at atmospheric-pressure and the APPJ efficiently uses power and precursor gas, it must still compete in quality with low-pressure systems used in industry. ATR FTIR shows almost identical spectra for both wafers etched using an APPJ and an industry ready ICP (see Fig. 6). It can be seen that no significant signal from the photoresist remains, and that using an APPJ can produce a surface that would be expected from current ashing solutions.

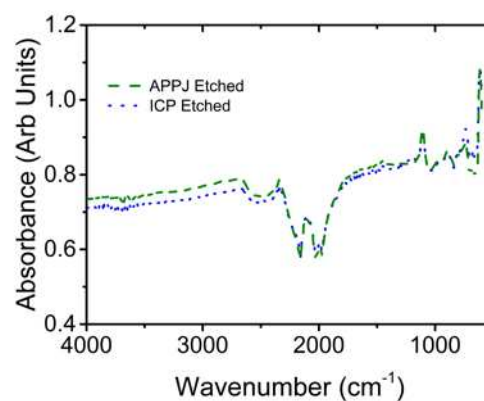


Fig. 6. ATR FTIR spectra for silicon wafers: unaltered, with photoresist (PR), and for wafers after the photoresist has been removed for both low-pressure plasma solutions and the atmospheric-pressure plasma.

#### 4. Conclusions

Removing photoresist using an APPJ can give fast removal rates with a quality comparable to current industry techniques. The removal of photoresist shows a strong relationship with atomic oxygen as has been postulated for low-pressure. Atomic oxygen has been measured using TALIF and shows trends matching that of etch rate for the same variations in parameters.

To further improve on the possible etch rate of  $10 \mu\text{m}/\text{min}$ , modelling can predict operating parameters and device designs that maximise the production of atomic oxygen, as well as designs that can overcome limitations such as flow rate and maximum power input.

The waste power dissipated by the whole RF system can be reduced by replacing off-the-shelf matching solutions with bespoke custom inductive components and shortening cable lengths. The treatment size of the device is just over 1 cm in diameter, and assuming a plasma power consumption of 5 W, the resulting requirement for a 6 inch wafer is  $\sim 200$  jets to checkerboard treat the surface for an energy cost of  $\sim 1 \text{ kW}$  at 100 times the speed of current low-pressure systems.

#### 5. Acknowledgements

The authors would like to thank the University of York for their support through a Teaching Studentship, and the UK EPSRC grant EP/K018388/1.

## 6. References

- [1] B. Thedjoisworo, D. Cheung and V. Crist. *J. Vacuum Sci. Technol. B: Microelectr. Nanometer Struct.*, **31**, 2 (2013)
- [2] D.M. Manos and D.L. Flamm. *Plasma Etching: An Introduction*. (1989)
- [3] V. Schulz-von der Gathen, V. Buck, T. Gans, N. Knake, K. Niemi, St. Reuter, L. Schaper and J. Winter. *Contr. Plasma Phys.*, **47**, 7 (2007)
- [4] V. Schulz-von der Gathen, L. Schaper, N. Knake, St. Reuter, K. Niemi, T. Gans and J. Winter. *J. Phys. D: Appl. Phys.*, **41**, 19 (2008)
- [5] E. Wagenaars, T. Gans, D. O'Connell and K. Niemi. *Plasma Sources Sci. Technol.*, **21**, 4 (2012)
- [6] K. Niemi, D. O'Connell, N. de Oliveira, D. Joyeux, L. Nahon, J.P. Booth and T. Gans. *Appl. Phys. Lett.*, **103**, 3 (2013)
- [7] N. Knake, S. Reuter, K. Niemi, V. SchulzVvon der Gathen and J. Winter. *J. Phys. D: Appl. Phys.*, **41**, 19 (2008)
- [8] N. Knake, K. Niemi, S. Reuter, V. Schulz-von der Gathen and J. Winter. *Appl. Phys. Lett.*, **93**, 13 (2008)
- [9] J. Waskoenig, K. Niemi, N. Knake, L.M. Graham, S. Reuter, V. Schulz-von der Gathen and T. Gans. *Plasma Sources Sci. Technol.*, **19**, 4 (2010)
- [10] T. Murakami, K. Niemi, T. Gans, D. O'Connell and W.G. Graham. *Plasma Sources Sci. Technol.*, **22**, 1 (2013)
- [11] M.A. Lieberman and A.J. Lichtenberg. *Principles of Plasma Discharges and Materials Processing, 2nd Edition*. (2005)
- [12] J.Y. Jeong, S.E. Babayan, V.J. Tu, J. Park, I. Henins, R.F. Hicks and G.S. Selwyn. *Plasma Sources Sci. Technol.*, **7**, 3 (1998)
- [13] L. Haijiang, W. Shouguo, Z. Lingli and Y. Tianchun. *Plasma Sci. Technol.*, **6**, 5 (2004)
- [14] S.X. Jia, L.L. Zhao, J.H. Yang, C. Zhang and S.G. Wang. *Appl. Mechanics Mat.*, **260** (2013)
- [15] K.H. Han, J.G. Kang, H.S. Uhm and B.K Kang. *Curr. Appl. Phys.*, **7**, 2 (2007)
- [16] D. Marinov and N.S.J. Braithwaite. *Plasma Sources Sci. Technol.*, **24**, 6 (2014)